

THE INVESTIGATION OF SPECTROSCOPIC AND THEORETICAL METHODS OF BISISOXAOLINE DERIVATIVE OF NORBORNADIEN

Kerem MESÇİ¹, Serpil ERYILMAZ^{2*}, Melek GÜL³, Ersin İNKAYA⁴

¹Department of Physics, Institute of Science, Amasya University, Amasya, TURKEY

²Department of Physics, Faculty of Arts and Sciences, Amasya University, Amasya, TURKEY

³Department of Chemistry, Faculty of Arts and Sciences, Amasya University, Amasya, TURKEY

⁴Central Research Laboratory, Amasya University, Amasya, TURKEY

ABSTRACT

In this study, the synthesis of bisisoxaoline derivative of norbornadien from heterocyclic compounds was performed via 1,3-dipolar cycloaddition reaction, the structural properties of derivative characterized by spectroscopic analysis such as FT-IR, ¹H-NMR, ¹³C-NMR, UV-Vis and the single-crystal X-ray diffraction technique. The 3,7-bis(4-(tert-butyl)phenyl)-3a,4,4a,7a,8,8a-hexahydro-4,8-methanobenzo[1,2-d:4,5-d']dioxazole compound was optimized using Density Functional Theory (DFT/B3LYP) method with 6-311G(d,p) basis set in the ground state and the geometric parameters compared with single-crystal X-ray diffraction technique. The compound crystallizes in the monoclinic space group *C2/c* with *a* = 20.634(4) Å, *b* = 11.179(2) Å, *c* = 11.0690(17) Å and *Z* = 4 unit cell parameters. Also, the spectral results were examined with calculated vibrational frequencies, ¹H-NMR, ¹³C-NMR chemical shift values and absorption wavelengths, theoretically. The energetic behaviour of the compound in different solvent media was examined with TD-DFT/B3LYP method and 6-311G(d,p) basis set using the Conductor Polarizable Continuum Model (CPCM). The frontier molecular orbitals (FMOs), molecular electrostatic potential (MEP) and electronic structure parameters (dipole moment, electronegativity, chemical hardness-softness, ionization potential, electron affinity, etc.) were examined to get information about the chemical stability of the structure.

Keywords: Bisisoxaoline, DFT, Single Crystal X-ray, FT-IR, NMR

1. INTRODUCTION

1,3-dipolar cycloaddition is not only powerful tool for the synthesis of five membered heterocyclic compounds, but also generated new chiral centres [1]. In recent years, the isoxazoline compounds were obtained from nitrile oxides via 1,3-dipolar cycloaddition reaction since they are significant role in organic and pharmacologically active compounds. The moiety of isoxazoline has been found in various biological activities. Bicyclic isoxazoline derivative which is GABA analogues (1), is known to exhibit anticonvulsant activity [3]. The Lee 878 (2) compound is effective of antimicrobial against of *Mycobacterium tuberculosis* [4]. The biologically active isoxazoline derivatives are shown in Figure 1. Lee and co-workers have been found antituberculosis activity of organic compounds as a core unit of isoxazoline groups [5].

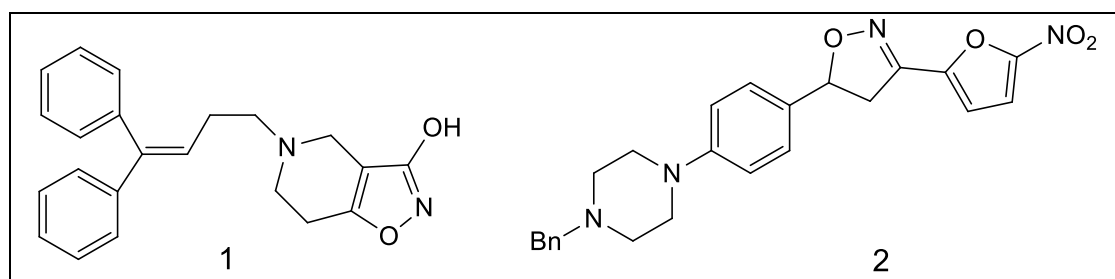


Figure 1. Biologically active Isoxazoline derivatives

*Corresponding Author: srpleryilmaz@gmail.com

Nitrile oxide compounds were obtained from aldoxime via one-pot reaction. Aromatic aldehyde was converted aldoxime compounds before were treated NaOCl to obtained hydroximoyl chloride followed dehydrohalogenation [6].

In literature, some isoxazoline compounds of 2,5-norbornadiene derivatives are include as mono-dipolar cycloaddition reaction [7]. We haven't found any data about one-pout domino cycloaddition reaction of 2,5-norbornadiene with nitrile oxides.

So, we examined structural properties of the *3,7-bis(4-(tert-butyl)phenyl)-3a,4,4a,7a,8,8a-hexahydro-4,8-methanobenzo[1,2-d:4,5-d']diisoxazole* compound with spectroscopic and theoretical methods. The chemical structure of the synthesized compound was characterized with FT-IR, ¹H-NMR, ¹³C-NMR, UV-Vis and the single-crystal X-ray diffraction technique.

The theoretical molecular geometry parameters, vibrational frequencies, chemical shift and absorbance wavelength values were compared with the experimental results. The energetic behaviour of the compound in different solvent media was examined. In addition, physical and chemical properties of the compound were investigated by frontier molecular orbital energies and dipole moment, electronegativity, chemical hardness-softness etc. electronic structure parameters.

2. MATERIAL AND METHODS

2.1. Synthesis Process

In this study, we synthesized an isoxazoline derivatives of according to the structure of 2,5-norbornadiene, which is include symmetrically two double bond, for use domino cycloaddition reaction. We have recently reported reaction condition of nitrile oxide addition via dipolar cycloaddition reaction [8]. Under the reaction conditions, the nitrile oxides cycloaddition reaction was investigated for the domino cycloaddition. The reaction condition is shown in Figure 2. Further shorten the reaction time to 3 hours; yield was observed increasing under ultrasound system as green chemical method. When the reaction performed with a *4-tert-butylbenzaloxime* (3.3 mmol) and 2,5-norbornadiene (1 mmol), the reaction provided the domino cycloaddition product (**3**) in 85% yield. We determined that treatment of the *4-tert-butylbenzaldehyde* with hydroxylamine hydrochloride which gave aldoxime compounds. The purification of aldoxime compounds via column chromatography and the crystallization with chloroform.

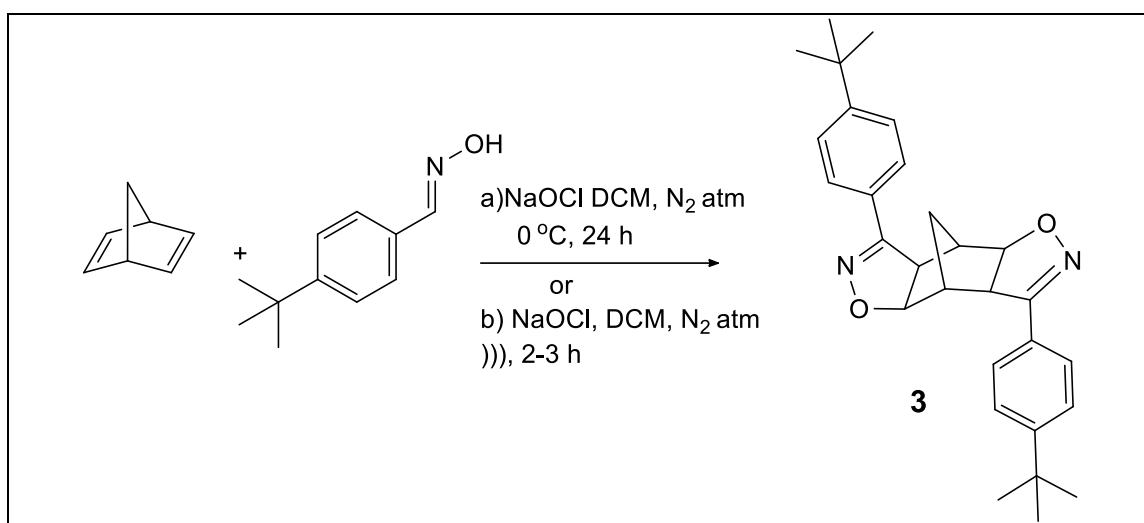


Figure 2. Domino cycloaddition reaction condition.

A three-neck round bottomed flask was charged with the appropriate 2,5-norbornadiene (1 equiv), aldoxime (3.3 equiv), and anhydrous DCM (5 mL) was the mixture sonicated with started drop wise NaOCl (2.5 equiv) added via syringe, under N₂ for 0.5 hours until TLC (1:2, EtOAc: hexanes) dedicated completion of aldoxime. The reaction mixture was extracted three times with diethyl ether and brine. The residue was purified directly by column chromatography to give the desired isoxazoline.

Compound (3):

3,7-bis(4-(*tert*-butyl)phenyl)-3a,4,4a,7a,8,8a-hexahydro-4,8-methanobenzo[1,2-d:4,5-d']diisoxazole.

Colourless crystals, 85% yield, m.p. 128°C, R_f = 0.41 (1:2, ethyl acetate/n-hexane).

FT-IR [KBr/(cm⁻¹)]: 2956.20, 2927, 2865.3, 1609.11, 1591.7, 1514.5, 1409.57, 1394.9, 1361.12, 1248.2, 1112.95, 904.72, 888.11, 835.93.

¹H-NMR (400 MHz, CDCl₃) δ: δ 7.64 (m, 4H H7, H9, H7ⁱ ve H9ⁱ), 7.45 (d, *J* = 8.4 Hz, 4H, H6, H10, H6ⁱ ve H10ⁱ), 4.84 (d, *J* = 8.2 Hz, 1H, H12), 4.75 (d, *J* = 8.3 Hz, 1H, H12ⁱ), 3.83 (d, *J* = 8.3 Hz, 1H, H13), 3.65 (d, *J* = 8.2 Hz, 1H, H13ⁱ), 2.95 (brs, 2H, H14, H14ⁱ), 1.59 (d, *J* = 6.2 Hz, 2H, H15a,b), 1.34 (s, 18H, *tert*-butyl) ppm.

¹³C-NMR (100 MHz, CDCl₃) δ: 155.62, 155.50, 153.72, 153.61, 126.64, 126.49, 125.87, 125.79, 125.54, 86.36, 83.27, 56.77, 52.85, 50.78, 46.06, 34.89, 31.16, 26.96 ppm.

LC-MS: C₂₉H₃₄N₂O₂ (m/z) 442.26.

2.2. Experimental Details and Spectroscopic Analysis Instruments

All the reaction materials used were commercially available and use drying DCM over CaH₂. Ultrasound assisted reactions were carried out using a Bandelin ultrasound with 35 kHz frequency. IR spectra was obtained with a "Perkin Elmer, FT-IR" system and reported in terms of frequency of absorption (cm⁻¹). Melting point was determined on a capillary point apparatus equipped with digital thermometer, "Thermo". NMR spectra were determined with a "Bruker Ac-400 MHz NMR". TMS (tetramethylsilane) was used as an internal standard and CDCl₃ was used as the solvent. Signal multiplicities in the NMR spectra were reported as follows: s-singlet, brs-broad singlet, d-doublet, dd-doublet of doublets, m-multiplet. Elemental analysis was determined by Leco-Truspec CHNS Elemental analyzer. Mass spectrometer was measured with AB-Sciex LC-MS/MS-QTrap. The compound has been identified in the AUMAULAB Central Laboratory in Amasya University in Turkey.

2.3. X-ray Crystallography

The single-crystal X-ray data was collected on a Bruker D8 QUEST diffractometer. All diffraction measurements were performed at room temperature (296 K) using graphite monochromated Mo-K α radiation ($\lambda = 0.71073 \text{ \AA}$). Reflection data was recorded in the rotation mode using the ω scan technique by using X-AREA software [9]. Unit cell parameters were determined from least-squares refinement of setting angles with θ in the range $3.5 \leq \theta \leq 22.4$. The structure was solved by direct methods using SHELXS-97 [10] implemented in WinGX [11] program suit. The refinement was carried out by full-matrix least-squares method on the positional and anisotropic temperature parameters of the non-hydrogen atoms or equivalently corresponding to 191 crystallographic parameters, using SHELXL-97 [12]. Data collection: X-AREA, cell refinement: X-AREA, data reduction: X-RED32 [13]. The general purpose crystallographic tool PLATON [14] was used for the structure analysis and presentation of the results. The molecular graphic were done using ORTEP-3 for Windows [11]. Details of the data collection conditions and the parameters of the refinement process are given in Table 1.

Table 1. Crystal data and structure refinement parameters for the (3) compound

CCDC deposition no.	1444550
Colour	Colourless
Chemical formula	C ₂₉ H ₃₄ N ₂ O ₂
Formula weight	442.58
Temperature (K)	296
Wavelength (Å)	0.71073 Mo-K α
Crystal system	Monoclinic
Space group	C2/c
Unit cell parameters	
<i>a</i> , <i>b</i> , <i>c</i> (Å)	20.634 (4), 11.179 (2), 11.0690 (17)
<i>B</i>	101.012 (5)
Volume (Å ³)	2506.2 (8)
<i>Z</i>	4
<i>D</i> _{calc} (g/cm ³)	1.173
μ (mm ⁻¹)	0.07
<i>F</i> (000)	952
Crystal size (mm ³)	0.13 × 0.09 × 0.08
Diffractometer/measurement method	Bruker D8 QUEST 2/ ω scan
Index ranges	-25 ≤ <i>h</i> ≤ 25, -13 ≤ <i>k</i> ≤ 13, -9 ≤ <i>l</i> ≤ 13
θ range for data collection (°)	3.5 ≤ θ ≤ 22.4
Reflections collected	14380
Independent/observed reflections	2468 / 1104
<i>R</i> _{int}	0.123
Refinement method	Full-matrix least-squares on <i>F</i> ²
Data/restraints/parameters	14380/0/150
Goodness-of-fit on <i>F</i> ²	1.02
$\Delta\rho_{\max}$, $\Delta\rho_{\min}$ (e/Å ³)	0.24, -0.24

2.4. Theoretical Calculations Process

All the theoretical analysis on the structure have been performed with Gaussian 09W [15] electronic structure and GaussView 5.0 [16] graphical interface programmes. Primarily, the initial molecular geometry of the compound (3) was taken on the coordinates obtained from the X-ray diffraction data and the optimization process was carried out DFT / B3LYP (Becke's Three Parameter Hybrid Functional using the Lee, Yang and Parr Correlation Functional) [17-19] method with 6-311G(d,p) the basis set in the ground state. And all theoretical calculations were made over the optimized structure and the same method. To examine the IR spectral character of the compound (3), harmonic vibrational frequencies were calculated and to eliminate systematic errors between the experimental values and theoretical

values the frequencies multiplied by the scale 0.9682 [20]. ^1H and ^{13}C -NMR chemical shift values were calculated according to GIAO (Gauge-Independent Atomic Orbital) method [21], and also TMS (tetramethylsilane) which an internal standard chemical shifts, as solvent CDCl_3 . To examine the impact of the solvent effect on electronic transitions in the UV-VIS spectral analysis, theoretical transition wavelengths are calculated at different solvent media such as dimethyl sulfoxide, tetrahydrofuran and methanol with Time Dependent TD/DFT using Conductor Polarizable Continuum Model (CPCM) [22] at the basis set 6-311G(d,p). The frontier molecular orbital energies-the highest energy occupied molecular orbital (HOMO) and the lowest unoccupied molecular orbital energy (LUMO)-have been calculated and provided very useful information in determining the energy and electronic transitions. Furthermore, molecular electrostatic potential (MEP) map and some structure parameters (the dipole moment, electronegativity, chemical hardness-softness, ionization potential, electron affinity, etc.) were examined using the same theoretical method in order to gain information about chemical reactivity of the compound (**3**).

3. RESULTS AND DISCUSSION

3.1. Description of the Single-Crystal Structure and Optimized Structure

The molecular structure of 3,7-bis(4-(*tert*-butyl)phenyl)-3a,4,4a,7a,8,8a-hexahydro-4,8-methanobenzo[1,2-d:4,5-d']diisoxazole with the atom numbering scheme is shown in Figure 3.a. The (**3**) molecule is monoclinic having space group $C2/c$, with four molecules in unit cell ($Z = 4$), with following dimensions $a = 20.634(4) \text{ \AA}$, $b = 11.179(2) \text{ \AA}$, $c = 11,0690(17) \text{ \AA}$ and $\beta = 101.012(5)^\circ$. The molecule resides on mirror symmetry located on the C15 atom.

The molecule is consists of four groups. One of them, which is important for our works, is isoxazole ring. The other groups are, bicyclic ring, phenyl ring and *tert*-butyl group. The isoxazole ring is planar with a maximum deviation of 0.0023 (11) \AA for atom C11. All bond lengths (C–C 1.496–1.539 \AA , C=N 1.281 \AA , C–O 1.454 \AA , and O–N 1.414 \AA) on the isoxazole ring are in the acceptable range and similar with literature value [8, 23]. The C=N bond length of 1.281 \AA confirms it's a double bond. The *tert*-butyl group C–C bond lengths C1–C4, C2–C4 and C3–C4 are 1.534(6), 1.509(6) and 1.527(6), respectively. These lengths are similar with literature values [24]. The C–C bond lengths in the phenyl rings are observed in the range of 1.368(4)–1.389(3) \AA . The bond lengths are consistent with previously phenyl ring-containing studies [25].

In the investigated molecule, there are no remarkable intra-intermolecular hydrogen bond interactions. The molecule stabilized by weak Van der Waals forces.

The optimized structure of the (**3**) compound, as shown in Figure 3.b. was obtained over the geometry formed by crystallographic data, some selected geometric parameters (such as bond lengths and angles, torsion angles) were compared with experimental values and the results were tabulated in Table 2.

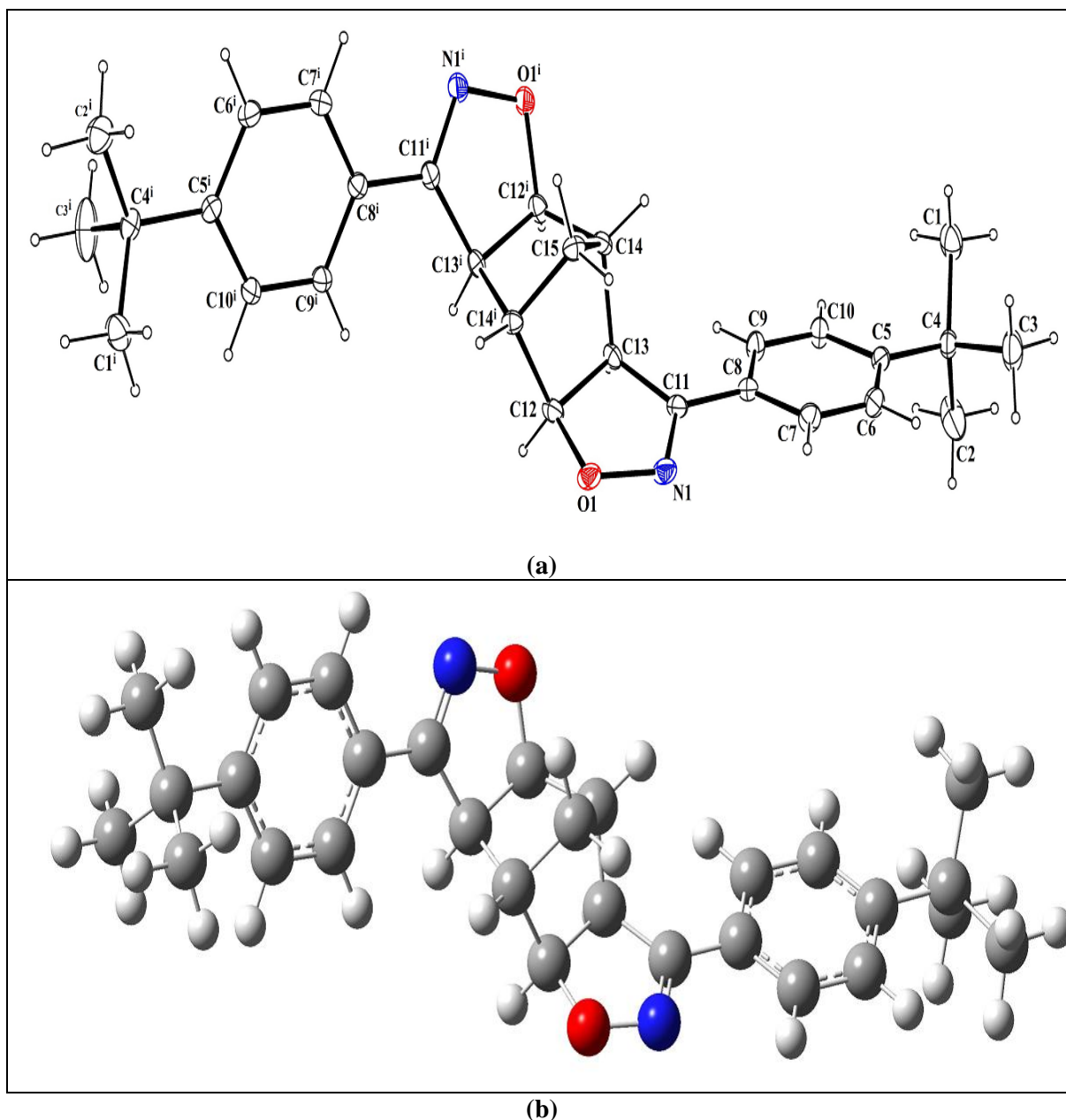


Figure 3. a) An ORTEP-3 view of the (3) compound showing the atom-numbering scheme. Displacement ellipsoids are drawn at the 20% probability level and H atoms are shown as small spheres of arbitrary radii. b) The optimized geometric structure of the (3) compound with DFT/B3LYP method and 6-311G(d,p) basis set.

As can be seen from the Table 2, N1-C11, N1-O1, O1-C12 bond lengths are 1.281(4), 1.414(4), 1.454(4) Å experimentally, 1.284, 1.393, 1.451 Å theoretically. These values were indicated as 1.290, 1.383, 1.478 Å for 6-31G(d,p) basis set, 1.285, 1.380, 1.480 Å for 6-311+G(d,p) basis set [26], 1.285, 1.388, 1.453 Å for 6-311G(d,p) basis set [8], in other DFT studies on the isoxazole derivatives which performed by our group. Also C12-C13 and C11-C13 bond lengths are stated as 1.553, 1.514 Å, theoretically, and we can say that C=N, N-O, C-O, C-C bond lengths within the isoxazole ring are in agreement with both reported in similar paper and typical values (C=N 1.47 Å, N-O 1.40 Å C-O 1.43 Å, C-C 1.54 Å). C12-C13 bond length which connecting between isoxazole and bicyclic groups is the longest length and recorded as 1.539(4) Å experimental, 1.553 Å theoretical.

C12ⁱ-C13ⁱ bond length is shown similar result C12-C13 as 1.553 Å, and C12-C14ⁱ is related C12ⁱ-C14 as 1.538Å. These results are referred a mirror symmetry of the (3) compound.

Table 2. Some selected experimental and theoretical geometrical parameters of the (3) compound

<i>Parameters</i>	<i>Experimental Values</i>	<i>Theoretical Values</i>
	<i>(X-Ray Analysis)</i>	<i>DFT/6-311G(d,p)</i>
<i>Bond Lengths (Å)</i>		
N1-C11	1.281(4)	1.284
N1-O1	1.414(4)	1.393
O1-C12	1.454(4)	1.451
C12-C13	1.539(4)	1.553
C11-C13	1.496(5)	1.514
C8-C11	1.463(5)	1.469
C4-C5	1.518(5)	1.538
C13-C14	1.538(5)	1.558
C14-C15	1.529(5)	1.541
C15-C14 ⁱ	1.529(5)	1.541
C12-C14 ⁱ	1.519(5)	1.538
C14-C12 ⁱ	1.519 (5)	1.538
C1-H1A/H1B/H1C		1.093/1.092/1.094
C2-H2A/H2B/H2C	0.9600	1.092/1.094/1.093
C3-H3A/H3B/H3C		1.093
<i>Bond Angles (°)</i>		
C11-N1-O1	110.3(2)	110.8
N1-O1-C12	109.5(2)	110.1
N1-C11-C8	122.2(4)	121.2
N1-C11-C13	113.6(6)	113.4
O1-C12-C13	104.7(3)	104.9
C15-C14-C13	102.3(2)	102.1
C9-C8-C11	120.3(4)	121.1
C15-C14-H14	115.0	117.0
H15A-C15-H15B	110.3	108.9
O1-C12-C14 ⁱ	111.0(3)	111.5
C12 ⁱ -C14-C13	106.5(3)	105.6
C14-C15-C14 ⁱ	94.5(4)	94.9
C14 ⁱ -C12-C13	103.9	103.9
<i>Torsion Angles (°)</i>		
C11-N1-O1-C12	3.4(4)	2.7
O1-N1-C11-C8	-177.3(3)	-179.0
O1-N1-C11-C13	0.6(4)	0.5
N1-O1-C12-C13	-5.7(3)	-4.6
N1-C11-C13-C14	106.1(3)	106.5
N1-C11-C13-C12	-4.0(4)	-3.2
O1-C12-C13-C11	5.6(3)	4.5
O1-C12-C13-C14	-113.7(3)	-115.0
N1-O1-C12-C14 ⁱ	-177.2(3)	-116.5
C14 ⁱ -C12-C13-C11	122.1(3)	121.7
C11-C13-C14-C12 ⁱ	177.2(3)	178.4
C12 ⁱ -C14-C15-C14 ⁱ	55.78(19)	55.19

The C12ⁱ-C14-C13 and C14-C15-C14ⁱ bond angles of bicyclic ring, which has sp³ hybridized one carbon bridge, are observed as 106.5(3), 94.5(4)° experimental, while these angles are 105.6, 94.9° according to DFT/B3LYP/6-311G(d,p) method. The bond angle between on bridge atoms is stated 93.8° in other study [8]. In view that, mirror symmetry is not only bond length also bond angles, for example C12-C14ⁱ-C13ⁱ and C12ⁱ-C14-C13 as 105.6°.

We should mention that are minor differences between the experimental and theoretical parameters, because compound is accepted in the gas phase during theoretical calculation process, whereas it is solid

phase in the experimental analysis, and molecules connected to each other with hydrogen bonds in this phase. Figure 4 is shown a global comparison was performed the atom-by-atom superimposition obtained from X-ray diffraction and the theoretical calculations and RMSE value is 0.903 Å. Also, we examined correlation coefficients to determine relationships or compliance between experimental and theoretical values. R^2 value is 0.9679 for bond lengths, 0.9850 for bond angles, and correlation graphics are shown in Figure 5.

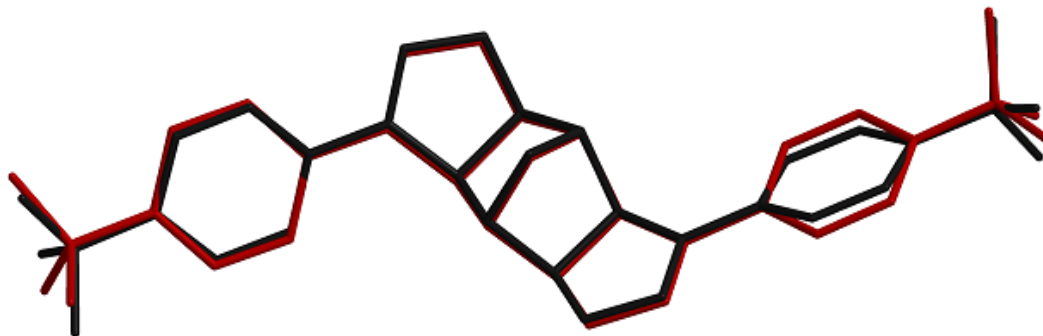


Figure 4. Atom-by-atom superimposition of the calculated structure (DFT/B3LYP76-311G(d,p) (red) on the X-ray structure (black) of the (3) compound

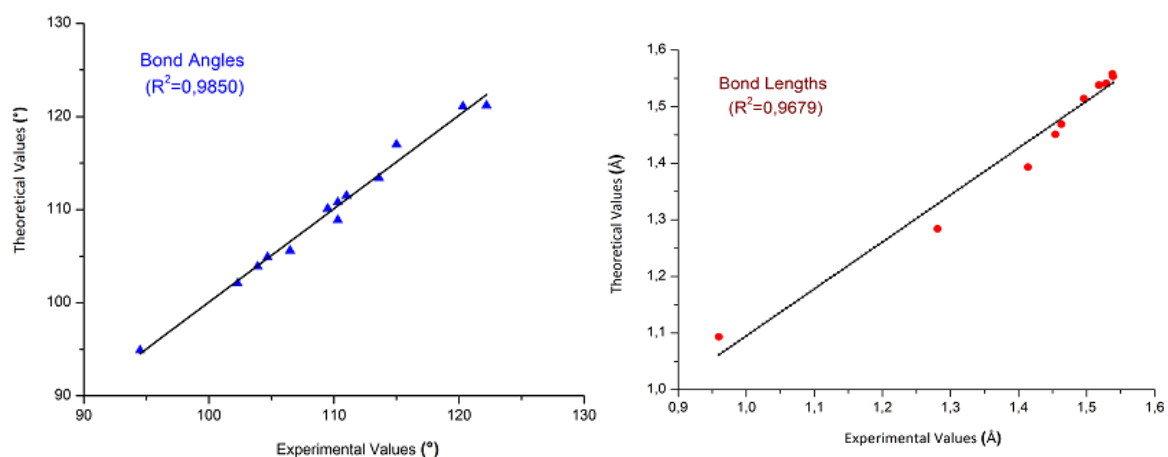


Figure 5. The correlation graphics for geometric parameters of the (3) compound

3.2. Vibrational Spectral Analysis

The scaled harmonic vibrational frequencies were calculated with DFT/B3LYP/6-311G(d,p) basis set to determine characteristic functional groups of the (3) compound. The experimental FT-IR spectrum which plotted on the transmittance (%) against the wavenumber (cm^{-1}) is shown in Figure 6.

The (3) compound, which has 67 atoms and 195 fundamental vibrational frequencies, consists isoxazole moiety, bicyclic ring, phenyl and *tert*-butyl groups. The stretching and bending vibrational assignments in these groups were designated with Gauss View interface program [16], compared with spectral values and results tabulated in Table 3.

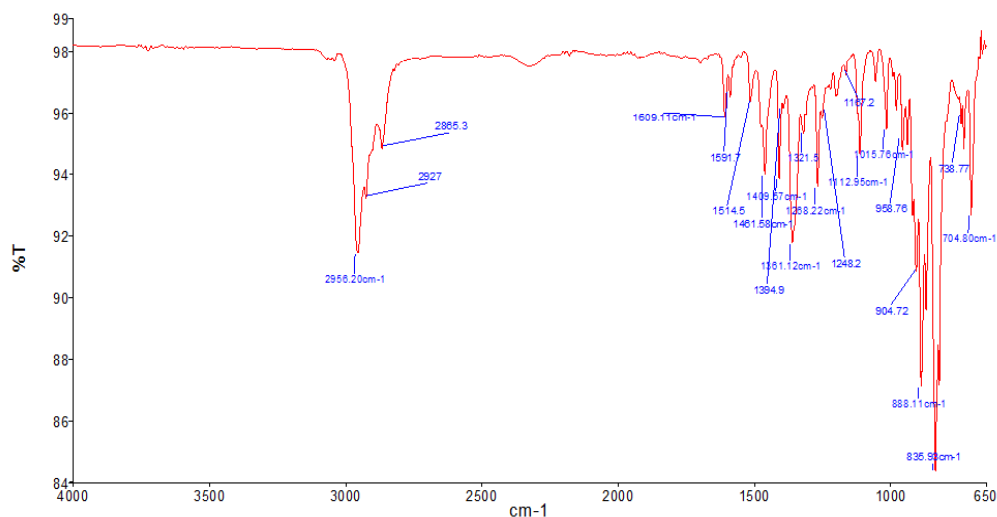


Figure 6. FT-IR spectrum of the (3) compound.

Table 3. Comparison of the experimental and theoretical vibrational spectra analysis of the (3) compound

<i>Assignment</i>	<i>Experimental FT-IR (cm⁻¹) with KBr</i>	<i>Calculated (scaled) (cm⁻¹) B3LYP/6-311G(d,p)</i>
$\nu_s(\text{C-H})_{\text{phenyl}}$	2956.2	3104.6
$\nu_{\text{as}}(\text{C-H})_{\text{phenyl}}$	-	3089.6
$\nu_s(\text{C-H}_2)_{\text{bicyclic}}$	2927	2983.7
$\nu_{\text{as}}(\text{C-H})_{\text{bicyclic}}$	-	2965.8
$\nu_s(\text{C-H})_{\text{tert-butyl}}$	2865.3	2933.9
$\nu(\text{C=N})_{\text{isoxazole}}$	1609.1	1587.1
$\nu(\text{C-C})_{\text{phenyl}}$	1591.7	1538.9
$\gamma(\text{C-H})_{\text{phenyl}}$	1514.5	1498.6
$\alpha(\text{C-H}_3)_{\text{tert-butyl}}$	1409.5	1437.1
$\alpha(\text{C-H})_{\text{phenyl}}$	1394.9	1394.1
$\gamma(\text{C-H})_{\text{phenyl+ isoxazole}}$	1361.1	1330.2
$\omega(\text{C-H})_{\text{tert-butyl+ bicyclic}}$	1248.2	1235.4
$\delta(\text{C-H})_{\text{bicyclic}}$	1112.9	1100.8
$\beta(\text{CCC})_{\text{phenyl}}$	1015.7	998.9
$\nu(\text{N-O})_{\text{isoxazole}}$	958.7	921.4
$\theta_{\text{bicyclic+ isoxazole}}$	904.7	906.2
β_{bicyclic}	835.9	826.2
θ_{phenyl}	704.8	654.3

Vibrational modes: ν ; stretching (s; symmetric, as; asymmetric), γ ; rocking, α ; scissoring, ω ; wagging, δ ; twisting, β ; deformation, θ ; ring breathing.

The C-H stretching vibrations are observed at 2956.2-2865.3 cm^{-1} in the FT-IR spectrum, 3104.6-2933.9 cm^{-1} in the theoretical IR spectrum of the (3) compound. C-H stretching vibrations in phenyl ring-a typical C-H stretching in aromatic group-are recorded at 2956.2, 3104.6-3089.6 cm^{-1} , at 2927, 2983.7-2965.8 cm^{-1} in bicyclic ring, as spectral and theoretical values. These values are noticeable specific bands in this region and consistent with 3100-3000 cm^{-1} bandwidth which defined C-H stretching vibrational for cyclic ring and aromatic group [27]. The strong C-H stretching vibrational mode is recorded at 2865.3 cm^{-1} experimentally, 2933.9 cm^{-1} theoretically in *tert-butyl*, and the assignments are compatible with the knowledge as strong and weak C-H stretching vibrations belong to methyl group are recorded about 2960-2850 cm^{-1} wavenumber [28, 29]. In the other isoxazole studies, C=N stretching band which is characteristic of the isoxazole ring vibrations are observed 1589.6, 1588.3 cm^{-1} for 6-311G(d,p) [8], 1586, 1584 cm^{-1} for 6-31G(d,p) and 1579 cm^{-1} for 6-311+G(d,p) basis set [26], while this band are recorded at 1609.1 and 1587.1 cm^{-1} in this study, experimental and computed values,

respectively. C-H in-plane and out-of plane bending vibrations bands belong to functional groups of the (3) compound are recorded at 1514.5-1112.9 cm^{-1} for spectral and from 1498.6 to 1100.8 cm^{-1} for theoretical values. And, N-O stretching vibration mode is predicted at 921.4 cm^{-1} , while this mode is stated at 878 and 879 cm^{-1} in a isoxazolone [30], 977 cm^{-1} [31] and 923.2-912-6 cm^{-1} [8] in isoxazole studies. The deformation modes on the functional groups and whole structure are observed in the values below at 906.2 cm^{-1} . We think that predicted vibrational modes and computed frequencies are in compliance with experimental values and similar papers in literature. To make comparison theoretical with experimental results, we have examined correlation graphic and correlation coefficient (R^2 value is 0.9984), correlation graphic shown in Figure 7.

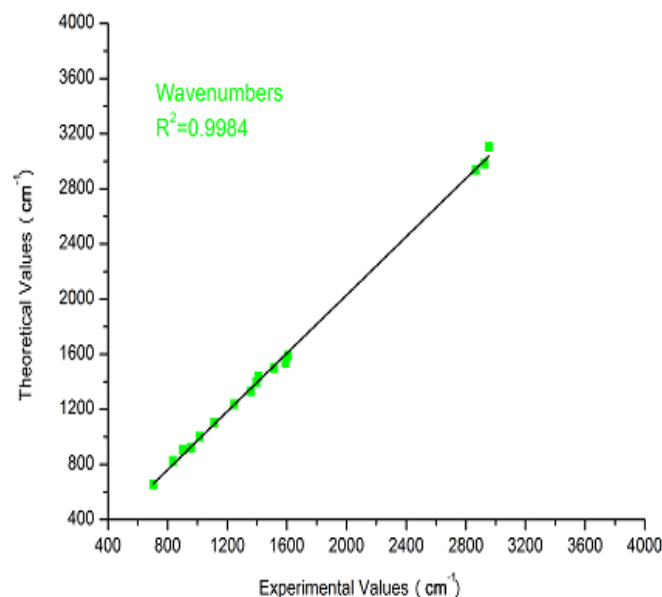


Figure 7. The correlation graphic for experimental and theoretical wavenumbers of the (3) compound

3.3. NMR Spectral Analysis

Spectral and theoretical ^{13}C -NMR and ^1H -NMR chemical shifts values of the (3) compound were recorded within the range of 155.62-26.96 ppm, 163.34-30.18 ppm and 7.64-1.34 ppm, 8.37-1.09 ppm respectively, and these values belong to atoms are shown in Table 4.

As can be seen in the Table 4, C11 atom, which is the bridge atom among the isoxazole and phenyl groups, with the highest chemical shift value in the downfield was observed at 155.62 ppm, 163.34 ppm for as experimental, theoretical, respectively. So, C11ⁱ chemical shift value is 155.50 ppm another highest value. Because the (3) compound has a mirror symmetry and some chemical shift values are very close together for symmetric atoms.

sp^2 hybridized C11 atom having double bond with nitrogen, has shifted in downfield because of decrease of the electron density and weak shielding effect. The phenyl ring atoms, C6, C7, C8, C9 and C10, have chemical shift values special to aromatic ring carbon atoms (100-150 ppm) [32, 33]. They were recorded 126.64-125.54 ppm as experimental, 133.66-130.97 ppm as theoretical. Although C5 atom is a phenyl ring atom, it has slightly higher chemical shift value (153.72 ppm) than the other ring carbon atoms since has substituent of the *tert-butyl*.

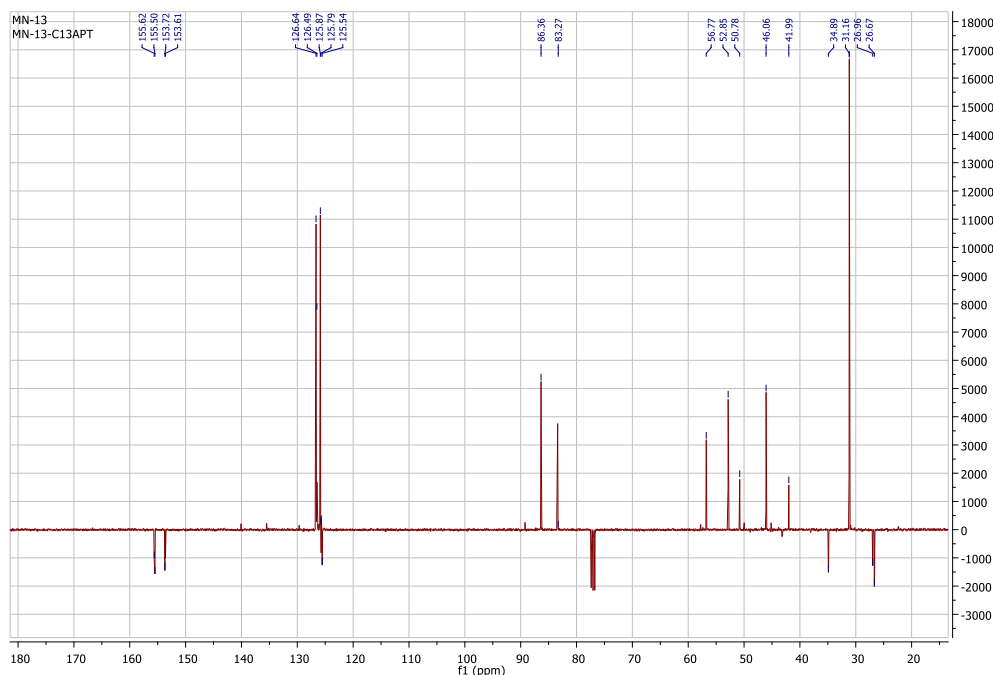
The chemical shift values are belong to aromatic hydrogen H6, H7, H9 and H10 atoms are 7.64-7.45 ppm as spectral values, 8.37 and 7.56 ppm as computed values with GIAO method. These resonance values are in accord with the literature [34] that indicates as 6.0-8.5 ppm for aromatic protons. The H12 atom has higher chemical shift value (4.88 ppm experimentally, 4.92 ppm theoretically) than H13 atom

due to attached electronegative oxygen atom. The *tert-butyl* protons have given low chemical shift values in the up field, these values are confirm that information sp^3 hybridized methyl group protons are assigned at 0-2 ppm [28].

^{13}C -NMR and ^1H -NMR spectrums of the (3) compound are shown in Figure 8. To compare the experimental and theoretical values, the correlation graphics were examined, R^2 value is 0.9985 for ^{13}C -NMR, 0.9936 for ^{13}C -NMR shown in Figure 9.

Table 4. Experimental and theoretical ^{13}C -NMR and ^1H -NMR isotropic chemical shift values for the (3) compound

Atom	Experimental chemical shift values (ppm)/ CDCl_3	Theoretical chemical shift values (ppm)/B3LYP	Atom	Experimental chemical shift values (ppm)/ CDCl_3	Theoretical chemical shift values (ppm)/B3LYP
C1/ C1 ⁱ	31.16	34.70	C14/C14 ⁱ	50.78/46.06	53.06
C2/ C2 ⁱ	31.16	30.18	C15	26.96	30.18
C3/ C3 ⁱ	31.16	34.72	H1/H1 ⁱ	1.34	1.15-1.20-1.63
C4/ C4 ⁱ	34.89	42.20	H2/H2 ⁱ	1.34	1.09-1.54-1.56
C5/C5 ⁱ	153.72/153.61	162.47	H3/H3 ⁱ	1.34	1.13-1.18-1.64
C6/C6 ⁱ	125.54	130.97	H6/H6 ⁱ	7.45	7.57
C7/C7 ⁱ	125.79	132.41	H7/H7 ⁱ	7.64	8.37
C8/C8 ⁱ	126.49	133.48	H9/H9 ⁱ	7.64	7.56
C9/C9 ⁱ	125.87	132.74	H10/H10 ⁱ	7.45	7.80
C10/C10 ⁱ	126.64	133.66	H12/H12 ⁱ	4.84/4.75	4.92
C11/C11 ⁱ	155.62/155.50	163.34	H13/H13 ⁱ	3.83/3.65	3.56
C12/C12 ⁱ	86.36/83.27	94.44	H14/H14 ⁱ	2.95	2.89
C13/C13 ⁱ	56.77/52.85	58.95	H15a/H15b	1.59	1.51



a)

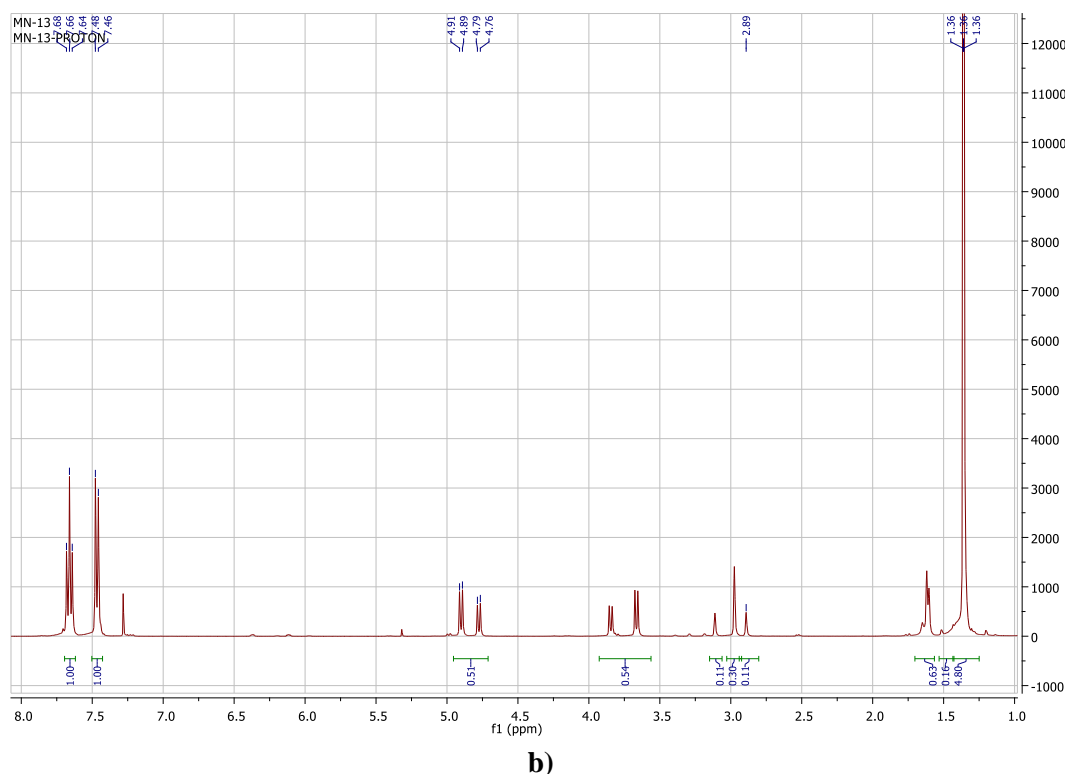


Figure 8. a) ^{13}C -NMR, b) ^1H -NMR spectrum of the (3) compound

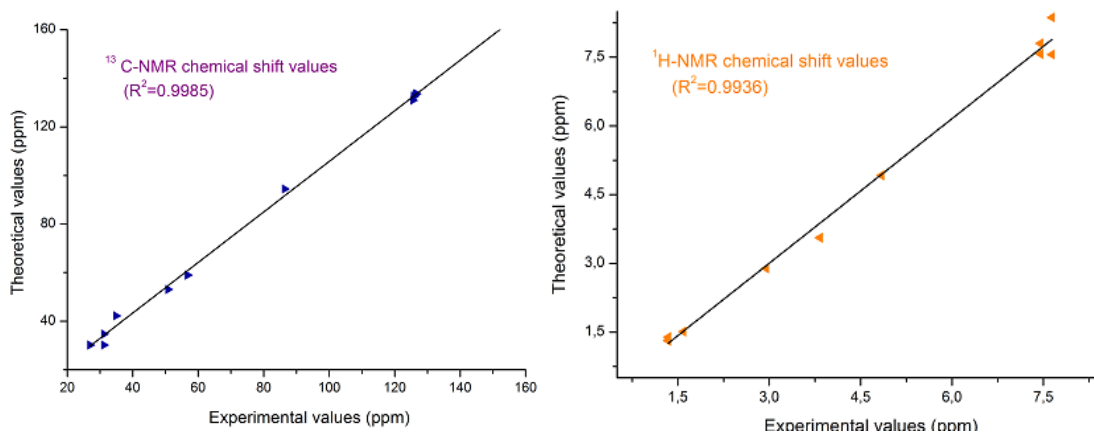


Figure 9. The correlation graphics for experimental and theoretical chemical shift values of the (3) compound

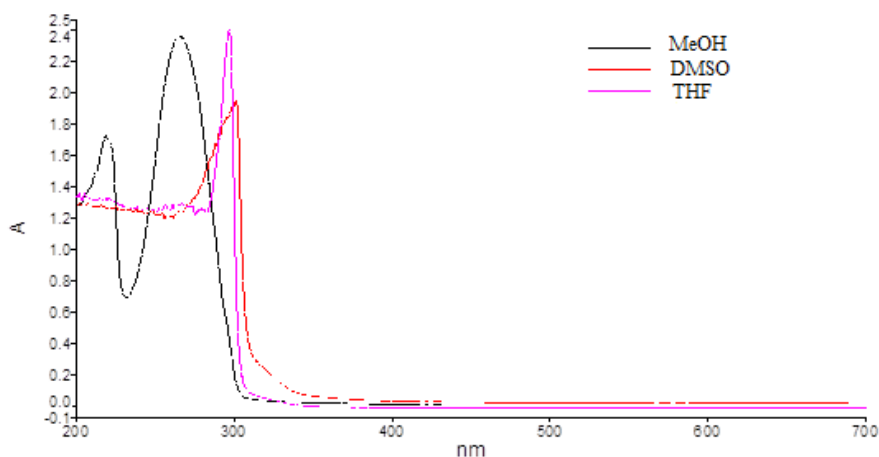
3.4. UV-Vis Spectral and FMOs Analysis

UV-Vis spectral analysis of the (3) compound was realized with TD-DFT/B3LYP/6-311G(d,p) in gas phase and different solvent media such as DMSO, THF and methanol. The absorption wavelengths which recorded as spectral result and theoretical prediction, excitation energies (eV) and oscillator strengths (f) are listed in Table 5. The electronic absorption spectrum which obtained in three different solvent is given Figure 10. The effect solvent which has different polarity are showed the effect maximum absorption wavelengths values, for instance; methanol is a polar and protic solvent and transitions are observed at lower wavelengths.

Table 5. The experimental and calculated UV-Visible parameters of the (3) compound

	<i>Experimental Wavelength</i> λ_{max} (nm)	<i>Theoretical Wavelength</i> λ_{max} (nm)	<i>Excitation Energy</i> (eV)	<i>Oscillator Strength</i> (f)	<i>Probable Orbital Transition</i>
<i>Gas Phase</i>		295.77	4.19	0.001	HOMO→LUMO(97%) HOMO-1→LUMO(55%)
		284.90	4.35	0.021	HOMO→LUMO+1(43%)
		280.75	4.41	1.172	HOMO-1→LUMO(42%) HOMO→LUMO+1(54%)
<i>THF</i>	392.9	296.48	4.18	0.001	HOMO→LUMO(98%)
	295.7	284.97	4.35	0.024	HOMO-1→LUMO(56%) HOMO→LUMO+1(42%)
	274.4	282.04	4.39	1.205	HOMO-1→LUMO(42%) HOMO→LUMO+1(55%)
<i>MeOH</i>	265.25	296.05	4.18	0.013	HOMO→LUMO(97%)
	221.99	284.91	4.35	0.022	HOMO-1→LUMO(55%) HOMO→LUMO+1(43%)
	217.02	281.39	4.40	1.183	HOMO-1→LUMO(42%) HOMO→LUMO+1(55%)
<i>DMSO</i>	379.80	296.38	4.18	0.001	HOMO→LUMO(98%)
	300.29	284.92	4.35	0.029	HOMO-1→LUMO(57%) HOMO→LUMO+1(41%)
	270.20	282.13	4.39	1.204	HOMO-1→LUMO(40%) HOMO→LUMO+1(57%)

The maximum absorption wavelengths values are related to $n \rightarrow \pi^*$ transition of around isoxazole moiety probably due to the presence of carbon-nitrogen double bond, other wavelengths can be concerned with $\pi \rightarrow \pi^*$ transitions of aromatic groups.

**Figure 10.** UV-Vis spectrum of the (3) compound

Frontier molecular orbitals' energies of the (3) compound were obtained using B3LYP method with 6-311G(d,p) basis set. The highest occupied molecular orbital-HOMO and the lowest unoccupied molecular orbital-LUMO and HOMO-1, LUMO+1 distributions for the structure and energy values are shown in Figure 11.

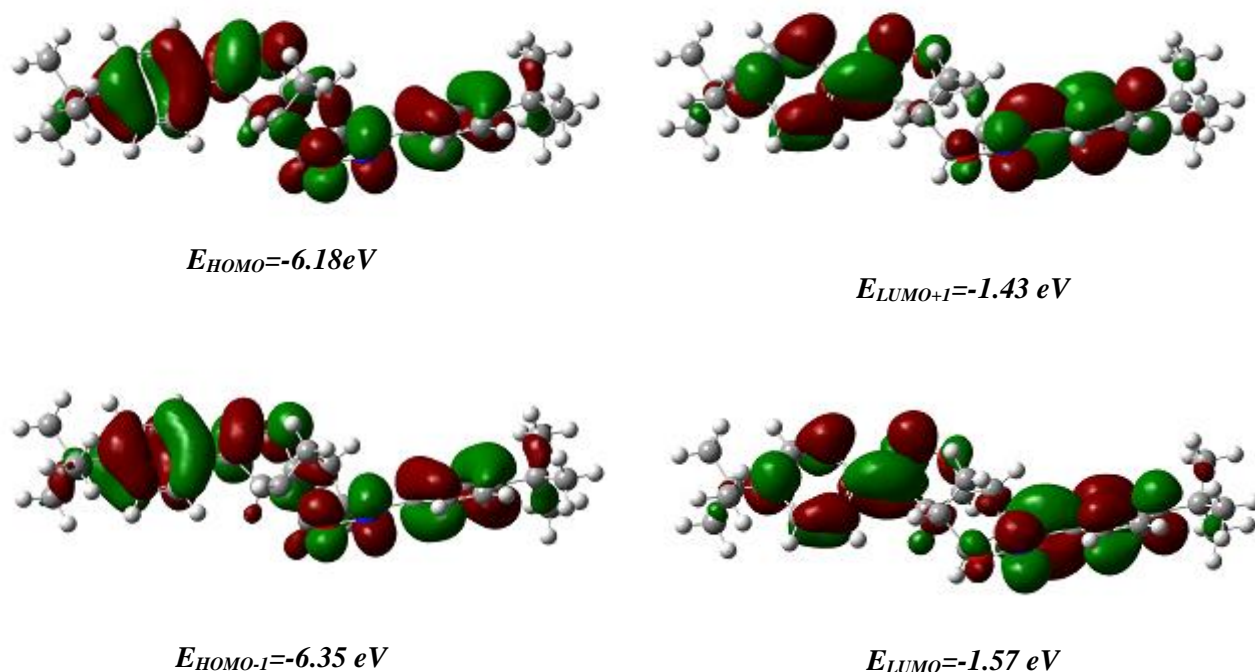


Figure 11. The frontier molecular orbitals and energy levels of the (3) compound in gas phase

The positive and negative phases seen in this Figure 11, which are red and green colour distributions and represent these phases in molecular orbital wave function, are distributed symmetrically over the whole structure except *tert-butyl* group. HOMO has located at the isoxazole moiety and phenyl groups, perhaps a little around bicyclic atoms but asymmetrically and except methylene group on the bridge. LUMO has settled over the isoxazole moiety and phenyl groups is quite satisfactory symmetrical for all positive and negative phases but excluding bicyclic ring. So, energy value of the band gap is calculated as $\Delta E = E_{HOMO} - E_{LUMO} = 4.61$ eV and it means that the compound has quite stable feature [35, 36].

HOMO has a nucleophilic characteristic which can donate electron, while LUMO can be acceptor electron as it has an electrophilic characteristic. HOMO-LUMO analysis helps to determinate electrical and optical properties for the chemical reactions, electrical transport properties and the state electronic transition at the UV-Vis spectra [8, 37, 38]. We benefited from these orbitals' energy values when examining the chemical reactivity features of the (3) compound in different solvent media. In addition, HOMO-LUMO energy values are used in calculation of the global reactivity descriptors which act as a bridge between stability of the structures and global chemical reactivity [8, 39]. Also this information about fundamental properties of the chemical reactivity such as ionization potential, electron affinity, electronegativity, chemical potential, global hardness and global softness etc. [40]. Energy values belong to frontier molecular orbitals can be considered as the important starting point to determine these parameters.

The ionization potential is the minimum energy required to remove an electron from an atom or molecule and can be expressed as, $I = -E_{HOMO}$ (I ; vertical ionization potential for DFT method). According to Koopman's Theory [41], electron affinity (A) is described as the change in energy when is an electron added to a neutral atom in the gas phase and is given as, $A = -E_{LUMO}$. Electronegativity (χ) and chemical hardness (η) [42, 43] help to predict about the formation of chemical bonds and the physical, chemical properties of the compound [44], can be calculated as $\chi = (I + A)/2$ and $\eta = (I - A)/2$. Similarly, other global reactivity descriptors are chemical softness (s) [44], electronic chemical potential (μ) as characteristic of electronegativity of compounds [41b, 45] and electrophilicity index (ω) [46] which defined as $s = 1/2\eta$, $\mu = -(I + A)/2$, $\omega = \mu^2/2\eta$, respectively. All of these concepts, total energies, dipole moments were

computed at gas phase ($\epsilon=1$) and at tetrahydrofuran ($\epsilon=7.42$), methanol ($\epsilon=32.63$), dimethyl sulfoxide ($\epsilon=46.82$) phase for UV-Vis region, the results are given in Table 6.

Table 6. The total energies, dipole moments and some global reactivity features of the (3) compound

	Gas ($\epsilon=1$)	THF ($\epsilon=7.42$)	MeOH ($\epsilon=32.61$)	DMSO ($\epsilon=46.82$)
E_{TOTAL}	-1385.62839088	-1385.62661374	-1385.62834116	-1385.62868789
μ_{Dipole}	2.9151	2.7256	2.9025	2.9193
E_{HOMO}	-6.1814	-6.1618	-6.1795	-6.1812
E_{LUMO}	-1.5789	-1.5618	-1.5776	-1.5789
I	6.1814	6.1618	6.1795	6.1812
A	1.5789	1.5618	1.5776	1.5789
χ	3.8801	3.8618	3.8785	3.8800
η	2.3012	2.3000	2.3009	2.3011
s	0.2172	0.2173	0.2173	0.2172
μ	-3.8801	-3.8618	-3.8785	-3.8800
ω	3.2711	3.2420	3.2688	3.2711

Total Energy (a.u), Dipole Moment (debye), Ionization potential (eV), Electron affinity (eV), Electronegativity (eV), Chemical hardness (eV), Chemical softness (eV⁻¹), Electronic chemical potential (eV), Electrophilicity index (eV)

It can be seen from Table 6 that the total energy of the (3) compound decreases with increasing polarity of the solvent, as dipole moment, other structure parameters and stability of the compound increases accordingly applied CPCM method.

3.5. Molecular Electrostatic Potential Analysis

The molecular electrostatic potential map of the (3) compound was generated at the B3LYP/6-311G(d,p) level. In that map, the region of the most negative electrostatic potential represents in red, blue the most positive electrostatic potential and green zero potential [47]. MEP helps with electrophilic and nucleophilic attack character of the molecules; namely, negative regions-red coloured are associated with electrophilic, and positive regions-blue coloured with nucleophilic attack.

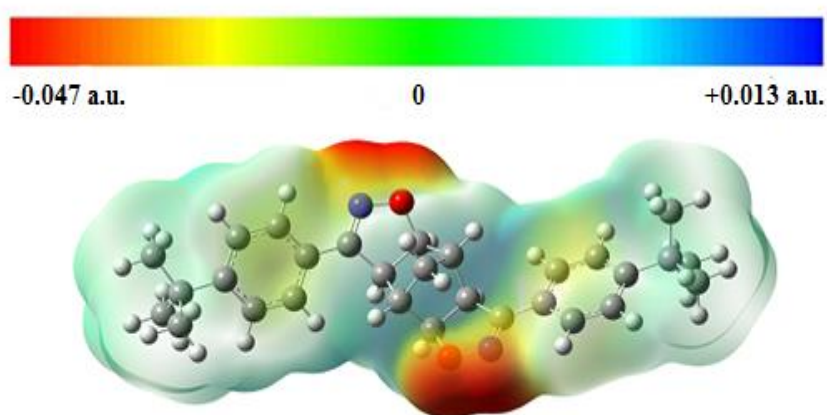


Figure 12. The molecular electrostatic potential map of the (3) compound

The MEP of the title compound is given in Figure 12, which has colour codes from red to blue, represents a potential distribution in the range of -0.047 a.u. to 0.013 a.u. The values of negative electrostatic potential are located on around isoxazole moiety, particularly nitrogen (with -0.0313 a.u.) and oxygen atoms (with -0.0326 a.u.), which are preferred site for electrophilic attack, while positive electrostatic

potential around bicyclic group, especially hydrogen atoms (with 0.0034 a.u.), which is preferred site for nucleophilic attack.

4. CONCLUSION

3,7-bis(4-(*tert*-butyl)phenyl)-3a,4,4a,7a,8,8a-hexahydro-4,8-methanobenzof[1,2-d:4,5-d']diisoxazole compound which is one of the bisisoxaoline derivative of norbornadien, synthesized and characterized with spectral analysis by FT-IR, ¹H-NMR, ¹³C-NMR, UV-Vis and X-ray crystallographic technique. The theoretical investigation were performed with DFT/B3LYP/6-311G(d,p) basis set over the ground state. And, the results of spectral analysis were compared with computed molecular geometric parameters, vibrational frequencies, ¹H-NMR and ¹³C-NMR chemical shifts. The theoretical geometric structure parameters such as bond lengths and angles, computed frequencies and chemical shifts values are in compliance with experimental values and similar papers or other isoxazole studies [8, 23, 26, 30, 31]. And also, electronic absorption spectrum analysis of the (**3**) compound was examined both experimental and with TD-DFT/B3LYP/6-311G(d,p)/CPCM methods in gas phase and different solvent media such as DMSO, THF and MeOH. The total energy, dipol moment and chemical stability parameters get changed with the different solvent polarity.

Also, we evaluated molecular geometry of isoxazoline ring position; *exo-endo*. The experimental NMR results have showed symmetrical same cyclo-addition such as both ring *exo-exo* or *endo-endo*, so we have described *exo* molecular geometry depend on spin-spin interaction on ¹H-NMR values. X-ray analysis results showed *exo* molecular geometry position and the comparisons with optimized geometry are reported in this work.

FMOs, MEP and thermodynamic analysis were realized to obtained information about nucleophilic or electrophilic characteristic, chemical activity properties such as ionization potential, electron affinity, electronegativity, chemical potential, global hardness and global softness, electronic transition at the UV-Vis spectra, electrostatic potential distribution on the molecule surface of the title compound. We hope that these consequences will create an infrastructure for researchers carrying out other isoxazole derivatives or similar studies and can be used for further analyses.

ACKNOWLEDGMENTS

This study was financially supported by the Amasya University Research Fund (Project No:FMB-BAP 054/085). The (**3**) compound has been identified in the AUMAULAB Central Laboratory in Amasya University, Turkey. Also, the authors acknowledge Scientific and Technological Research Application and Research Center, Sinop University, Turkey, for the use of the Bruker D8 QUEST diffractometer.

REFERENCES

- [1] a) Padwa A. 1,3-Dipolar Cycloaddition Chemistry II. 3rd. Ed. New York, NY, USA: Wiley Press, 1984.
b) Padwa A. Synthetic Application of 1,3-dipolar Cycloaddition Chemistry Toward Heterocycles and Natural Products. 3rd. Ed. New York NY, USA: Wiley Press, 2001.
- [2] a)Kaur K, Kumar V, Sharma AK, Gupta GK. Isoxazoline containing natural products as anticancer agents: A Review. Eur J Med Chem. 2014; 77:121-33.
b)Pekka KP, Tuomas O, Mikael P, Jorma JP, Janne AI, Reino L, Juha TP. Design, Synthesis, and Biological Evaluation of Nonsteroidal Cycloalkane[d]isoxazole-Containing Androgen Receptor Modulators. J. Med Chem 2012; 55 (14): 6316–6327.
- [3] Bolvig T, Larsson OM, Pickering DS, Nelson N, Falch E, Krogsgaard-Larsen P, Schousboe A. Action of bicyclic isoxazole GABA analogues on GABA transporters and its relation to anticonvulsant activity. Eur J Pharmacol. 1999; 375(1-3):367-74.

- [4] Tangallapally RP, Yendapally R, Daniels AJ, Lee REB, Lee RE. Nitrofurans as Novel Anti-tuberculosis Agents: Identification, Development and Evaluation. *Curr Top Med Chem* 2007; 7:509–526.
- [5] Rakesh DS, Lee RB, Tangallapally RP, Lee RE. Synthesis, optimization and structure–activity relationships of 3,5-disubstituted isoxazolines as new anti-tuberculosis agents. *Eur J Med Chem* 2009; 44:460–472.
- [6] Werner A. Über die Raumlische Anordnung der Atome in Stickstoffhaltigen Molekülen. *Berichte* 1890; 23:11-30.
- [7] a) Tranmer GK, Molybdenum WT. Mediated Cleavage Reactions of Isoxazoline Rings Fused in Bicyclic Frameworks. *Org. Lett* 2002; 4 (23): 4101–4104
b) Murphy JJ, Hamilton JG, Paton R M. Synthesis and ring opening metathesis polymerisation of isoxazolino and isoxazolidino-norbornenes. *Polymer* 2006; 47 (10): 3292-3297.
- [8] Eryılmaz S, Gül M, İnkaya E, İdil Ö, Özdemir Namik. Synthesis, Crystal Structure Analysis, Spectral Characterization, Quantum Chemical Calculations, Antioxidant and Antimicrobial Activity of 3-(4-chlorophenyl)-3a,4,7,7a-tetrahydro-4,7-methanobenzo[d]isoxazole. *J Mol Struct* 2016; 1122: 219-233.
- [9] Stoe&Cie, X-Area (Version 1.18), Stoe&Cie GmbH, Darmstadt, Germany, 2002.
- [10] Sheldrick GM. SHELXS-97. Program for the Solution of Crystal Structures. University of Gottingen. 1997.
- [11] Farrugia LJ. *J Appl Crystallogr* 1999; 30: 837-838.
- [12] Sheldrick GM. *Acta Crystallogr* 2015; C71: 3-8.
- [13] Stoe&Cie, X-RED (Version 1.04), Stoe&Cie GmbH, Darmstadt, Germany, 2002.
- [14] Spek AL. *Acta Crystallogr D* 2009; 65: 148-155.
- [15] Gaussian 09, Revision E.01, Frisch, M. J.; Trucks, G. W.; Schlegel, H. B.; Scuseria, G. E.; Robb, M. A.; Cheeseman, J. R.; Scalmani, G.; Barone, V.; Mennucci, B.; Petersson, G. A.; Nakatsuji, H.; Caricato, M.; Li, X.; Hratchian, H. P.; Izmaylov, A. F.; Bloino, J.; Zheng, G.; Sonnenberg, J. L.; Hada, M.; Ehara, M.; Toyota, K.; Fukuda, R.; Hasegawa, J.; Ishida, M.; Nakajima, T.; Honda, Y.; Kitao, O.; Nakai, H.; Vreven, T.; Montgomery, J. A., Jr.; Peralta, J. E.; Ogliaro, F.; Bearpark, M.; Heyd, J. J.; Brothers, E.; Kudin, K. N.; Staroverov, V. N.; Kobayashi, R.; Normand, J.; Raghavachari, K.; Rendell, A.; Burant, J. C.; Iyengar, S. S.; Tomasi, J.; Cossi, M.; Rega, N.; Millam, J. M.; Klene, M.; Knox, J. E.; Cross, J. B.; Bakken, V.; Adamo, C.; Jaramillo, J.; Gomperts, R.; Stratmann, R. E.; Yazyev, O.; Austin, A. J.; Cammi, R.; Pomelli, C.; Ochterski, J. W.; Martin, R. L.; Morokuma, K.; Zakrzewski, V. G.; Voth, G. A.; Salvador, P.; Dannenberg, J. J.; Dapprich, S.; Daniels, A. D.; Farkas, Ö.; Foresman, J. B.; Ortiz, J. V.; Cioslowski, J.; Fox, D. J. Gaussian, Inc., Wallingford CT, 2009.
- [16] GaussView, Version 5, Dennington, Roy; Keith, Todd; Millam, John. *Semichem Inc.*, Shawnee Mission, KS, 2009.
- [17] a) Becke AD. Density-functional exchange-energy approximation with correct asymptotic behavior. *J Chem Phys* 1988; 38: 3098-3100.
b) Becke AD. Density-Functional Thermochemistry. I. The Effect of the Exchange-Only Gradient Correction. *J Chem Phys* 1992; 96: 2155-2160.
c) Becke AD. Density functional thermochemistry III. The role of exact exchange. *J Chem Phys* 1993; 98: 5648-5652.

- [18] Ditchfield R, Hehre WJ, Pople JA. Self-Consistent Molecular-Orbital Methods. IX. An Extended Gaussian-Type Basis for Molecular-Orbital Studies of Organic Molecules *J Chem Phys* 1971; 54: 724-728.
- [19] Lee C, Yang CW, Parr R. Development of the Colle-Salvetti correlation-energy formula into a functional of the electron density. *Phys Rev* 1988; 37: 785–789.
- [20] Merrick JP, Moran D, Radom L. An Evaluation of Harmonic Vibrational Frequency Scale Factors. *J Phys Chem A* 2007; 111: 11683-11700.
- [21] a) London F. Théorie quantique des courants interatomiques dans les combinaisons aromatiques. *J Phys Radium* 1937; 8: 397-409.
b) McWeeny R. Perturbation Theory for the Fock-Dirac Density Matrix *Phys Rev* 1962; 126: 1028.
c) Ditchfield R. Self-consistent perturbation theory of diamagnetism. *Mol Phys* 1974; 27: 789-807.
d) Wolinski K, Hilton JF, Pulay P. Efficient implementation of the gauge-independent atomic orbital method for NMR chemical shift calculations. *J Am Chem Soc* 1990; 112: 8251-8260.
e) Cheeseman JR, Trucks GW, Keith TA, Frisch MJ. A comparison of models for calculating nuclear magnetic resonance shielding tensors. *J Chem Phys* 1996; 104: 5497-5509.
- [22] Barone V, Cossi M. Quantum calculation of molecular energies and energy gradients in solution by a conductor solvent model. *J Phys Chem A* 1998; 102: 1995-2001.
- [23] Jin YX, Zhong AG, Ge CH, Pan FY, Yang JG, Wu Y, Xie M, Feng HW. A novel difunctional acylhydrazone with isoxazole and furan heterocycles: Syntheses, structure, spectroscopic properties, antibacterial activities and theoretical studies of (E)-N0 -(furan-2-ylmethylene)-5-methylisoxazole-4-carbohydrazide. *J Mol Struct* 2012; 1010: 190-196.
- [24] Tamer Ö, Avcı BS, Avcı D, Nebioğlu M, Atalay Y, Çoşut B. Synthesis, molecular structure, spectral analysis and nonlinear optical studies on 4-(4-bromophenyl)-1-tert-butyl-3-methyl-1H-pyrazol-5-amine: A combined experimental and DFT approach. *J Mol Struct* 2016; 1106: 89-97.
- [25] Dege N, Senyüz N, Batı H, Günay N, Avcı D, Tamer O, Atalay Y. The synthesis, characterization and theoretical study on nicotinic acid [1-(2,3-dihydroxyphenyl)methylidene]hydrazide. *Spectrochim Acta A* 2014; 120: 323-331.
- [26] Eryılmaz S, Gül M, İnkaya E, Taş M. Isoxazole Derivatives of Alpha-pinene Isomers: Synthesis, Crystal Structure, Spectroscopic Characterization (FT-IR/NMR/GC-MS) and DFT Studies. *J Mol Struct* 2016; 1108: 209-222.
- [27] Mohan J. *Organic Spectroscopy: Principles and Applications*. 2nd Ed. Harrow, UK: Alpha Science, 2004.
- [28] Erdik E. *Organik Kimyada Spektroskopik Yöntemler*. 5. Baskı. Ankara, Türkiye: Gazi Kitabevi, 2008.
- [29] Stuart BH. *Infrared Spectroscopy: Fundamentals and Applications*. 1st Ed. Chichester, England: Wiley 2004.
- [30] Zhang XH, Zhan YH, Chen D, Wang F, Wang LY. Merocyanine dyes containing an isoxazolone nucleus: Synthesis, X-ray crystal structures, spectroscopic properties and DFT studies. *Dyes and Pigment* 2012; 93: 1408-1415.
- [31] Jin RY, Sun X H, Liu YF, Long W, Chen B, Shen SQ, Ma HX. Synthesis, crystal structure, biological activity and theoretical calculations of novel isoxazole derivatives. *Spectrochim Acta A* 2016; 152: 226-232.

- [32] Kalinowski HO, Berger S, Braun S. Carbon-13 NMR Spectroscopy. 1st ed. Chichester, UK John Wiley&Sons, 1988.
- [33] Pihlaja K, Kleinpeter E. Carbon-13 Chemical Shifts in Structural and Stereochemical Analysis. 1st ed. USA: Wiley-VCH Publishers, 1994.
- [34] Balcı M. Nükleer Manyetik Rezonans Spektroskopisi. 2. Baskı. Ankara, Türkiye:ODTÜ Yayıncılık, 2004.
- [35] İnkaya E, Günnaz S, Özdemir N, Dayan O, Dinçer M, Çetinkaya B. Synthesis, spectroscopic characterization, X-ray structure and DFT studies on 2,6-bis(1-benzyl-1H-benzo[d]imidazol-2-yl)pyridine. Spectr Acta Part A 2013; 103: 255–263.
- [36] İnkaya E, Dinçer M, Ekici Ö, Çukurovalı A. N'-(2-methoxy-benzylidene)-N-[4-(3-methyl-3-phenyl-cyclobutyl)-thiazol-2-yl]-chloro-acetic hydrazide: X-ray structure, spectroscopic characterization and DFT studies. J Mol Struct 2012; 1026:117-126.
- [37] Fleming I. Frontier Orbitals and Organic Chemical Reactions. London, UK:Wiley, 1976.
- [38] Tarı GÖ, Gümüş S, Ağar E. Crystal structure, spectroscopic studies and quantum mechanical calculations of 2-[(3-iodo-4-methyl)phenylimino)methyl]-5-nitro thiophene. Spectromica Acta Part A 2015; 141: 119-127.
- [39] Vijayaraj R,Subramanian V, Chattaraj PK. Comparison of Global Reactivity Descriptors Calculated Using Various Density Functionals: A QSAR Perspective. J Chem Theory Comput 2009; 5(10): 2744–2753.
- [40] Padmanabhan J, Parthasarathi R, Elango M, Subramanian V, Krishnamoorthy BS, Gutierrez-Oliva S, Toro-Labbe A, Roy D R, Chattaraj PK. Multiphilic Descriptor for Chemical Reactivity and Selectivity. J. Phys. Chem. A 2007; 111: 9130-9138.
- [41]a)Koopmans T. Physica 1. 1933; 104.
b)Vektariene A, Vektaris G. J Svoboda.A theoretical approach to the nucleophilic behavior of benzofused thieno[3,2-b]furans using DFT and HF based reactivity descriptors. ARKIVOC 2009; vii: 311-329.
- [42] Mulliken RS. J Chem Phys 1934; 2: 782.
- [43] a)Pearson RG.Hard and Soft Acids and Bases. J Am Chem Soc1963; 85:3533-3539
b)Pearson RG. Hard and soft acids and bases, HSAB, part 1: Fundamental principles. J Chem Educ1968;45(9): 581.
c)Pearson RG. Maximum Chemical and Physical Hardness. J Chem Educ1999;2 (76): 267.
- [44] Pearson RG. Absolute electronegativity and hardness correlated with molecular orbital theory. Pro Nat Acad Scie 1986; 83: 8440-8441.
- [45] Parr RG, Pearson RG. Absolute hardness: companion parameter to absolute electronegativity. J Am Chem Soc 1983;105: 7512-7516.
- [46] Chattaraj PK, Sarkar U, Roy DR. Electrophilicity index. Chem Rev 2006; 106: 2065-2091.
- [47] İnkaya E, Dinçer M, Ekici Ö, Çukurovalı A. 1-(3-Methyl-3-mesityl)-cyclobutyl-2-(5-pyridin-4-yl-2H-[1,2,4]triazol-3-ylsulfanyl)-ethanone: X-ray structure, spectroscopic characterization and DFT studies. Spect Acta Part A 2013; 101: 218-227.